UC Irvine
UC Irvine Previously Published Works

Title

Compact and multi-view solid state neutral particle analyzer arrays on National Spherical Torus Experiment-Upgrade

Permalink

https://escholarship.org/uc/item/7hw7x94h

Journal

Review of Scientific Instruments, 87(11)

ISSN

0034-6748

Authors

Liu, D
Heidbrink, WW
Tritz, K
et al.

Publication Date

2016-11-01

DOI

10.1063/1.4959798

Copyright Information

Peer reviewed

Compact and multi-view solid state neutral particle analyzer arrays on National Spherical Torus Experiment-Upgrade

D. Liu,[1,a)] W. W. Heidbrink,[1] K. Tritz,[2] E. D. Fredrickson,[3] G. Z. Hao,[1] and Y. B. Zhu[1]
[1]*Departments of Physics and Astronomy, University of California, Irvine, California 92697, USA*
[2]*Departments of Physics and Astronomy, Johns Hopkins University, Baltimore, Maryland 21218, USA*
[3]*Princeton Plasma Physics Laboratory, Princeton, New Jersey 08543, USA*

A compact and multi-view solid state neutral particle analyzer (SSNPA) diagnostic based on silicon photodiode arrays has been successfully tested on the National Spherical Torus Experiment-Upgrade. The SSNPA diagnostic provides spatially, temporally, and pitch-angle resolved measurements of fast-ion distribution by detecting fast neutral flux resulting from the charge exchange (CX) reactions. The system consists of three 16-channel subsystems: t-SSNPA viewing the plasma mid-radius and neutral beam (NB) line #2 tangentially, r-SSNPA viewing the plasma core and NB line #1 radially, and p-SSNPA with no intersection with any NB lines. Due to the setup geometry, the active CX signals of t-SSNPA and r-SSNPA are mainly sensitive to passing and trapped particles, respectively. In addition, both t-SSNPA and r-SSNPA utilize three vertically stacked arrays with different filter thicknesses to obtain coarse energy information. The experimental data show that all channels are operational. The signal to noise ratio is typically larger than 10, and the main noise is x-ray induced signal. The active and passive CX signals are clearly observed on t-SSNPA and r-SSNPA during NB modulation. The SSNPA data also indicate significant losses of passing particles during sawteeth, while trapped particles are weakly affected. Fluctuations up to 120 kHz have been observed on SSNPA, and they are strongly correlated with magnetohydrodynamics instabilities. *Published by AIP Publishing.* [http://dx.doi.org/10.1063/1.4959798]

I. INTRODUCTION

Fast ions play a key role in plasma heating and current drive in fusion plasmas, but their confinement and transport are susceptible to plasma instabilities.[1,2] Accurate measurements of fast ion distribution in real space and velocity space are crucial for understanding and eventually controlling fast ion dynamics. Neutral particle analyzer (NPA)[3] is a valuable fast-ion diagnostic that measures fast ions which charge exchange with beam neutrals and/or background neutrals. Compared with other fast ion diagnostics, NPA diagnostic has excellent pitch angle ($v_\parallel/v$) resolution. During the last decade, solid state neutral particle analyzer (SSNPA) based on the absolute extreme ultraviolet (AXUV) silicon photodiodes from Opto Diode Corporation (formerly International Radiation Detectors, Inc.)[4] has been successfully demonstrated in many magnetic fusion research facilities worldwide.[5–11] Compared with conventional NPA that uses parallel electric and magnetic fields as mass spectrometer, the SSNPA diagnostic is very attractive due to its compactness, cost-effectiveness, and easy handling features. The main limitations are that the SSNPA diagnostic cannot resolve the incident particle mass, and that x-ray and neutron/gamma ray induced noise could limit the performance in high temperature plasmas.

A new compact and multi-view SSNPA system, based on the design in Ref. 12, has been developed and tested on the National Spherical Torus Experiment-Upgrade (NSTX-U).[13] NSTX-U is a mid-size spherical tokamak equipped with two NB lines that contain six deuterium neutral beam (NB) sources with tangential radii of 50, 60, 70, 110, 120, and 130 cm. The NB injection energy is 65–90 keV, and total power can be up to 12 MW. In addition to NBs, NSTX-U will also use high harmonic fast wave (HHFW) for plasma heating. The new SS-NPA system aims at providing useful information on fast ion distribution in real space and velocity space, fast ion transport in the presence of instabilities, and fast ion acceleration by HHFW. In the rest of the paper, the hardware setup and main features are briefly described in Section II, and experimental data are discussed in Section III.

II. HARDWARE SETUP AND MAIN FEATURES

The NPA diagnostic relies on the charge exchange (CX) reactions of fast ions and neutral particles. Depending on the setup geometry, the CX neutrals can come from two sources: active component from the CX reactions with beam neutrals and passive component from the CX reactions with background neutrals especially the edge neutrals. The SSNPA diagnostic on NSTX-U has three subsystems at Bay B, I, and L near the equatorial plane which give radial and tangential active views, and a passive reference view (see Fig. 1). They are named as r-SSNPA, t-SSNPA, and p-SSNPA, respectively. The sightlines of r-SSNPA and t-SSNPA intersect with one of the
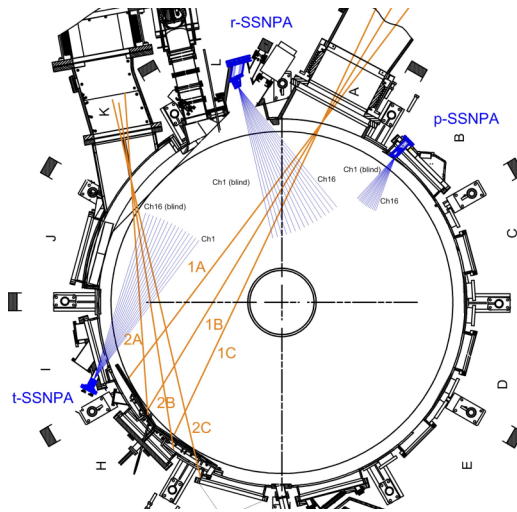

FIG. 1. Top down view of NSTX-U with six NB sources (1A, 1B, and 1C from NB line #1 and 2A, 2B, and 2C from NB line #2) and sightlines of three SSNPA subsystems located at Bay B, I, and L.
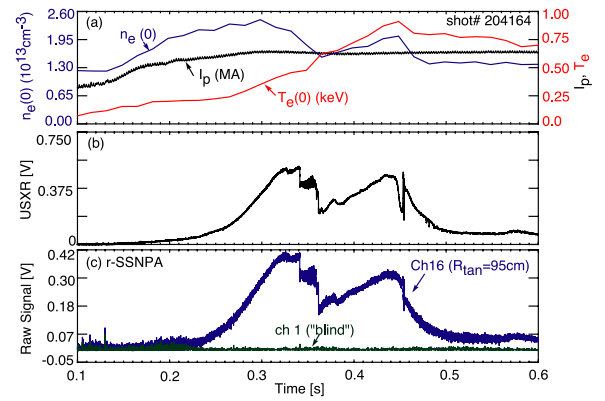

FIG. 2. Temporal evolution of (a) plasma current, core electron temperature, and core electron density, (b) soft x-ray, and (c) channel 16 (blue curve) and "blind" channel (green curve) of r-SSNPA in the Ohmic discharge #204164.

two NB lines, and their signals are mainly from the active CX signals. The p-SSNPA misses both NB lines, and it provides passive CX signals for reference. The primary detectors are 16-channel arrays of silicon diodes with directly deposited filter, a customized version of AXUV16ELG from Opto Diode Corporation.[4] For the t-SSNPA and r-SSNPA subsystems, three photodiode arrays are vertically stacked, and each array is coated with a thin filter of different thicknesses. Since the incident neutrals lose energy in the filters, it provides crude energy resolution through variation of the cutoff energy. The filters are mainly composed of tungsten with thicknesses of 100, 200, and 300 nm, and the corresponding low energy thresholds for a deuteron are ~25, ~45, and ~65 keV, respectively. The passive reference subsystem p-SSNPA has only one array with 100 nm filter due to the port size limitation. Because of the high atomic number, the tungsten filters are expected to block visible light and low energy soft x-ray, but remain transparent to energetic neutrals. In addition, the sightline of one channel of each detector array is blocked to monitor the electromagnetic (EM) and neutron/gamma induced noise. The SSNPA system is designed for a spatial resolution of ~5 cm.

The SSNPA electronics mainly consists of front-end transimpedance amplifiers, 2nd stage voltage amplifiers, and a D-Tacq digitizer ACQ196PCI-96-500 with sampling rate of 500 kHz. To minimize noise pick-up, the transimpedance amplifiers with EM shielding are directly plugged into the electrical feedthroughs without any cable. The 2nd stage voltage amplifier is placed close (~3 ft) to the detectors and drives analog signal to the D-Tacq digitizer through a twisted and shielded cable. The combination of front-end transimpedance amplifier and 2nd stage voltage amplifier gives a total gain of ~10^5 V/A and bandwidth of ~120 kHz. It is worth mentioning that proper grounding and good shielding are crucial to obtain clean signals during plasma operations. It is especially important to keep the shielding and the signal ground of transimpedance amplifiers at the same potential.

III. EXPERIMENTAL RESULTS AND DISCUSSION

A series of tests have been performed with the SSNPA system to check the data validity when the NSTX-U started the 2016 experimental campaign. The first test is to check EM, x-ray, and neutron/gamma induced noise. Fig. 2(c) shows the time traces of channel 16 (whose viewing area is the plasma core) and "blind" detector of r-SSNPA in an Ohmic discharge. Since there is no NB injection and thus no fast ion populations, no real CX signals are expected, and all signals are from either EM pick-up/interference, or background signal induced by X-ray or neutron/gamma radiation. As shown in Fig. 2(c), the EM noise and neutron/gamma induced noise (green curve) are typically small, but ~0.4 V unwanted signal is seen in channel 16 (blue curve) and other channels viewing the plasma core. Since the temporal evolution of this unwanted signal is strongly correlated with the soft x-ray signal, see Fig. 2(b), it is believed that the unwanted signal is caused by soft x-ray and hard x-ray. A survey with many Ohmic shots shows that only the channels that view the plasma core have relatively large unwanted signals, and other channels are much less affected. Because the plasma is typically hotter in the core, and the 100-300 nm thick tungsten filter mainly blocks low energy soft x-ray, not high energy soft x-ray and hard x-ray, this is expected. Based on the filter thickness, x-rays with energy larger than 1.5 keV could still have significant transmission. Generally, the x-ray induced noise can be roughly estimated with the soft x-ray signal and the correlation coefficient obtained from the Ohmic discharges. In NB heated plasmas, the x-ray induced noise is typically small, at least one order lower than the active CX signal. However, x-ray induced noise could be significant for the channels viewing the plasma core but missing the neutral beams. In those cases, background subtraction may be needed, and accurate subtraction requires to include the corrections for the geometry and the x-ray transmission curves of different systems.

The second test is to check the dependence of passive CX signals on the edge neutral density, since the CX neutral flux depends on the product of fast ion density and neutral density. On NSTX-U, one of the deuterium gas injectors is located at Bay I and very close to the t-SSNPA subsystem; thus this gas injector could be used to change the edge neutral density.
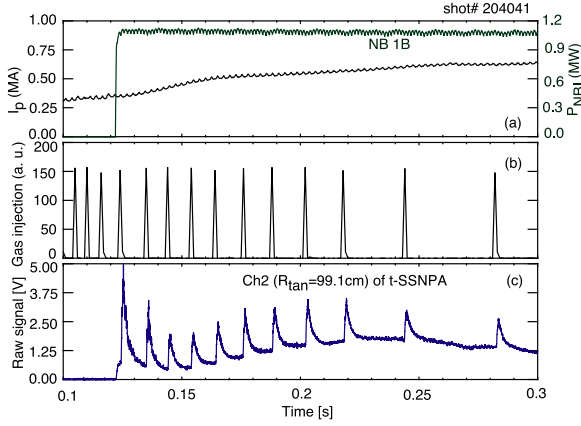
FIG. 3. Temporal evolution of (a) plasma current and NB power, (b) Bay I gas injection pulses, and (c) channel 2 of t-SSNPA.

Fig. 3(c) shows the signal from channel 2 of t-SSNPA in a NB heated discharge in which NB source 1B was injected at t = 0.122 s, and Bay I gas injector was used before t = 0.3 s. Since the viewing area of channel 2 does not intersect with the NB source 1B, the signal is dominated by the passive CX signals from the plasma edge. Figs. 3(b) and 3(c) clearly show that the bursts on passive CX signals of t-SSNPA are synchronized with the Bay I gas injection, and the bursts are generated by the increase of edge neutral density due to gas injection.
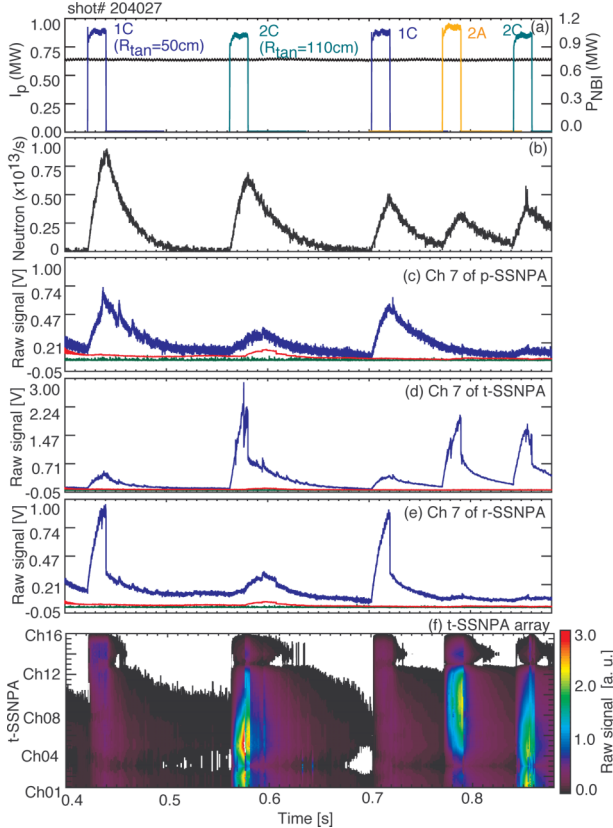

FIG. 4. Temporal evolution of (a) plasma current and injected NB power, (b) neutron rate, (c) channel 7 of p-SSNPA, (d) channel 7 of t-SSNPA, (d) channel 7 of f-SSNPA, and (f) one array of t-SSNPA. The "blind" detector signal and estimation of x-ray induced noise are also shown in (c)-(e) with green and red curves, respectively.
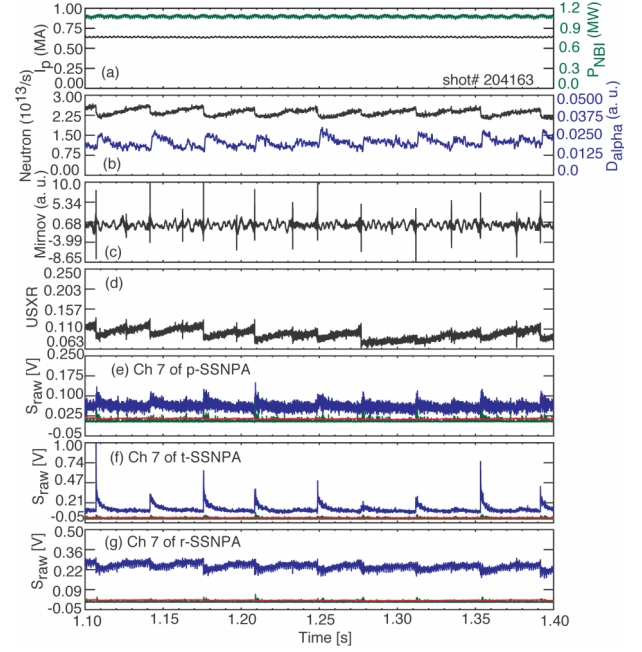

FIG. 5. Temporal evolution of (a) plasma current and injected NB power, (b) neutron rate and midplane D_{alpha}, (c) low frequency (<50 kHz) Mirnov signal, (d) soft x-ray, (e) channel 7 of p-SSNPA, (f) channel 7 of t-SSNPA, and (g) channel 7 of r-SSNPA. The "blind" detector signal and the estimation of x-ray induced noise are also shown in (e)-(g) with green and red curves, respectively.

The third test is to check the active and passive CX signals during neutral beam injection and after beam turn-off. Figs. 4(c)-4(f) show the SSNPA signals in a beam "blips" experiment in which ~20 ms pulses of NB source 1C, 2A, and 2C are alternatively injected. When 1C from NB line #1 is injected, r-SSNPA signals immediately increase, and then decays after the beam is turned off. Similarly, t-SSNPA signals jump up when NB 2A or 2C from NB line #2 is employed. Since the p-SSNPA system intersects with neither NB line #1 nor #2, the signals are purely passive signals, and they are weakly affected by the NB modulation.

The multi-view SSNPA system can separate the response of passing and trapped particles. The setup geometry determines that the active CX signals of t-SSNPA and r-SSNPA are sensitive to passing and trapped particles, respectively.[12] Fig. 5 shows the signals of three SSNPA subsystems in a time window with sawteeth indicated by Thomson data, neutron rate, Mirnov coil signal, and edge D_{alpha} emission. The bursts on t-SSNPA are the combined results of fast ions moving to the edge and increase in the edge neutral density. The r-SSNPA, which is mainly sensitive to trapped fast ions, shows only slight drops at each sawtooth. The data suggest that there are significant passing fast ion losses during sawteeth, while trapped particles are weakly affected.

The SSNPA system's fast time response also makes it possible to study fast ion density fluctuations in the presence of MHD instabilities. Fig. 6 shows that the SSNPA system observes fluctuations associated with 50-150 kHz TAE-like mode between t = 0.15-0.4 s and low frequency fishbone and kink modes after t = 0.47 s. The oscillations are observed in most channels of the three SSNPA subsystems but are absent in the "blind" detectors.
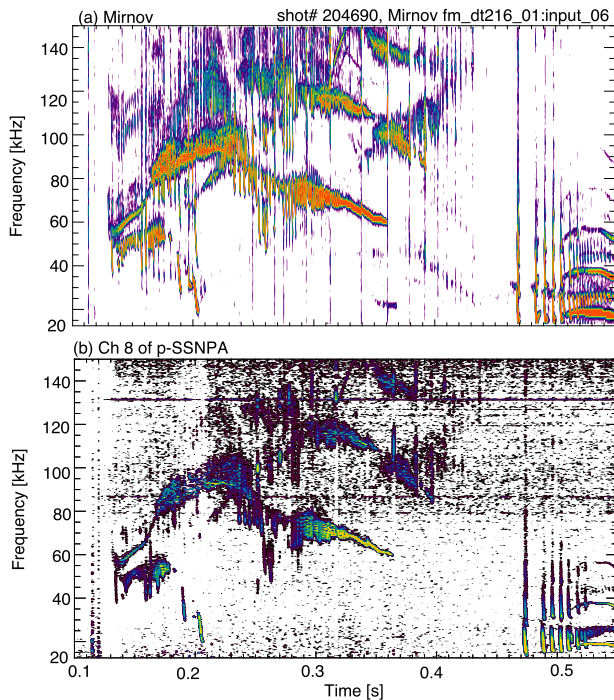
FIG. 6. Fourier spectrogram of (a) Mirnov coil measurement and (b) channel 8 of p-SSNPA.

IV. SUMMARY AND FUTURE WORK

The new SSNPA system has been successfully tested on the NSTX-U. Both active and passive CX signals are clearly observed on t-SSNPA and r-SSNPA during the NB modulation experiment. The SSNPA system has demonstrated the capability of separating the response of passing and trapped

particles and measuring the NPA flux fluctuations up to 120 kHz. In the next run campaign, a few individual detectors or an array will be added to work in pulse-counting mode to get fine energy spectrum, which is crucial for the study of the acceleration of fast ions by HHFW.

[1]W. W. Heidbrink and G. J. Sadler, Nucl. Fusion **34**, 535 (1994).
[2]A. Fasoli *et al.*, Nucl. Fusion **47**, S264 (2007).
[3]S. S. Medley, A. J. H. Donné, R. Kaita, A. I. Kislyakov, M. P. Petrov, and A. L. Roquemore, Rev. Sci. Instrum. **79**, 011101 (2008).
[4]See http://optodiode.com/products.html#IRD-UV-Photodiodes for more information about IRD AXUV silicon photodiode.
[5]K. Shinohara, D. S. Darrow, A. L. Roquemore, S. S. Medley, and F. E. Cecil, Rev. Sci. Instrum. **75**, 3640 (2004).
[6]E. Veshchev *et al.*, Rev. Sci. Instrum. **77**, 10F129 (2006).
[7]D. Liu, W. W. Heidbrink, D. S. Darrow, A. L. Roquemore, S. S. Medley, and K. Shinohara, Rev. Sci. Instrum. **77**, 10F113 (2006).
[8]V. Tang *et al.*, Rev. Sci. Instrum. **77**, 083501 (2006).
[9]Y. B. Zhu, A. Bortolon, W. W. Heidbrink, S. L. Celle, and A. L. Roquemore, Rev. Sci. Instrum. **83**, 10D304 (2012).
[10]R. Clary, A. Smirnov, S. Dettrick, K. Knapp, S. Korepanov, E. Ruskov, W. W. Heidbrink, and Y. Zhu, Rev. Sci. Instrum. **83**, 10D713 (2012).
[11]P. A. Schneider *et al.*, Rev. Sci. Instrum. **86**, 073508 (2015).
[12]D. Liu, W. W. Heidbrink, K. Tritz, Y. B. Zhu, A. L. Roquemore, and S. S. Medley, Rev. Sci. Instrum. **85**, 11E105 (2014).
[13]J. E. Menard *et al.*, Nucl. Fusion **52**, 083015 (2012).